Bisdonor–azaBODIPY–Fullerene Supramolecules: Syntheses, Characterization, and Light-Induced Electron-Transfer Studies

ARTICLE *in* THE JOURNAL OF PHYSICAL CHEMISTRY C · JANUARY 2014

Impact Factor: 4.77 · DOI: 10.1021/jp4112469

THE JOURNAL OF PHYSICAL CHEMISTRY C

Article

pubs.acs.org/JPCC

Bisdonor–azaBODIPY–Fullerene Supramolecules: Syntheses, Characterization, and Light-Induced Electron-Transfer Studies

Venugopal Bandi,[†] Mohamed E. El-Khouly,[‡,⊥] Kei Ohkubo,[‡] Vladimir N. Nesterov,[†] Melvin E. Zandler,[#] Shunichi Fukuzumi,*[,‡,§] and Francis D'Souza*[,†]

[†]Department of Chemistry, University of North Texas, 1155 Union Circle, #305070, Denton, Texas 76203-5017, United States

[‡]Graduate School of Engineering, Osaka University, ALCA, Japan Science and Technology Agency (JST), Suita, Osaka 565-0871, Japan

[#]Department of Chemistry, Wichita State University, 1845 Fairmount, Wichita, Kansas 67260-0051, United States

[§]Department of Bioinspired Science, Ewha Womans University, Seoul 120-750, Korea

Supporting Information

ABSTRACT: Achieving ultrafast light-induced charge separation requires carefully selected donor and acceptor entities often held together in a closer proximity. In the present investigation, two tetrads featuring a near-IR-emitting sensitizer, BF_2-chelated dipyrromethene (azaBODIPY), covalently linked to a fullerene through the central boron atom and two electron-donor entities, namely, *N*,*N*-dimethylaminophenyl, or bithiophene in close proximity to the fullerene entity were designed and synthesized, and the results were compared to the earlier-reported bisferrocene–azaBODIPY–fullerene tetrads in this series. The tetrads synthesized by establishing a multistep procedure exhibited typical spectral, redox, and photo reactivities of the individual components with some degree of intramolecular interaction. The X-ray structure of one of the precursor triads was also solved as part of this investigation. Ultrafast photoinduced electron transfer was witnessed in the case of both tetrads by femtosecond transient absorption spectroscopy studies. The significance of electron-donor entities was clear for the tetrad derived from *N*,*N*-dimethylaminophenyl entities, while for the bithiophene-derived tetrad, the charge separation involved mainly the azaBODIPY and fullerene entities. The charge recombination process involved populating the triplet excited state of azaBODIPY prior to returning to the ground state for both tetrads, as demonstrated by nanosecond transient absorption studies.

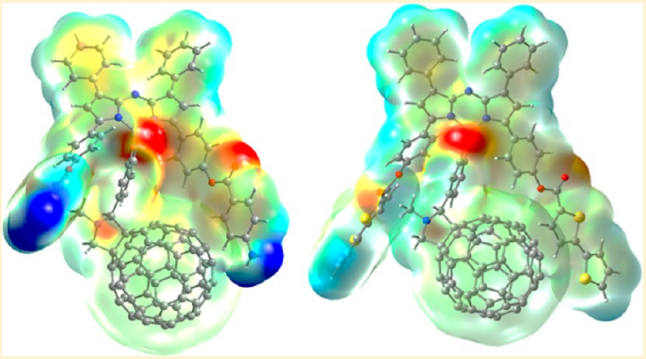

INTRODUCTION

Supramolecular multimodular donor–acceptor systems constructed using different photo- and redox-active species have been extensively investigated in the last 3 decades.[1−8] With suitably designed and assembled modular systems, these systems have found use in solar fuel and solar electricity generation and in building optoelectronic devices.[9−11] Traditionally, porphyrins and phthalocyanines have extensively been used as light-harvesting and electron-transfer units in these multimodular systems, performing photoinduced energy- and electron-transfer reactions.[3−7,12−14] Recently, BF_2-chelated dipyrromethene (BODIPY) dyes, derived from 4,4-difluoro-1,3,5,7-tetramethyl-4-bora-3a,4adiaza-*s*-indacene,[15] have emerged as efficient and tunable light-absorption and luminescent species. A large number of BODIPY derivatives can readily be obtained by modification of carbon positions at 1, 3, 5, 7, and 8,[15−17] exhibiting attractive photophysical characteristics with strong absorption bands in the visible region, making them comparable with those of porphyrins. Thus, nowadays, BODIPYs have been commonly employed to fulfill the role of light-harvesting antenna and electron-donor or -acceptor molecules.

BF_2-chelated azadipyrromethene (azaBODIPY) dyes are structural analogues of BODIPY dyes with nitrogen instead of carbon at the *meso*-position (position 8) of the BODIPY skeleton.[18] These dyes have attracted increasing attention because of their high extinction coefficients ($7-8 \times 10^5$ M^{-1} cm^{-1}), large fluorescence quantum yields, and small HOMO–LUMO gaps.[18,19] Consequently, they have been used in applications involving development of sensors, photodynamic therapy agents, and light-energy-harvesting systems.[20−22] With regard to the latter application, a few well-designed donor–acceptor systems have recently been designed/developed, and occurrences of photoinduced energy/electron transfer leading to a charge-separated state have been demonstrated.[21,22] Briefly, when azaBODIPY was connected to ferrocene, efficient

Received: November 15, 2013
Revised: January 9, 2014
Published: January 17, 2014

dx.doi.org/10.1021/jp4112469 | *J. Phys. Chem. C* 2014, 118, 2321−2332

Scheme 1. Structures of the Investigated azaBODIPY−Fullerene Dyad, 1, and Bisdonor−azaBODIPY−Fullerene (2−5) Supramolecular Tetrads[a]

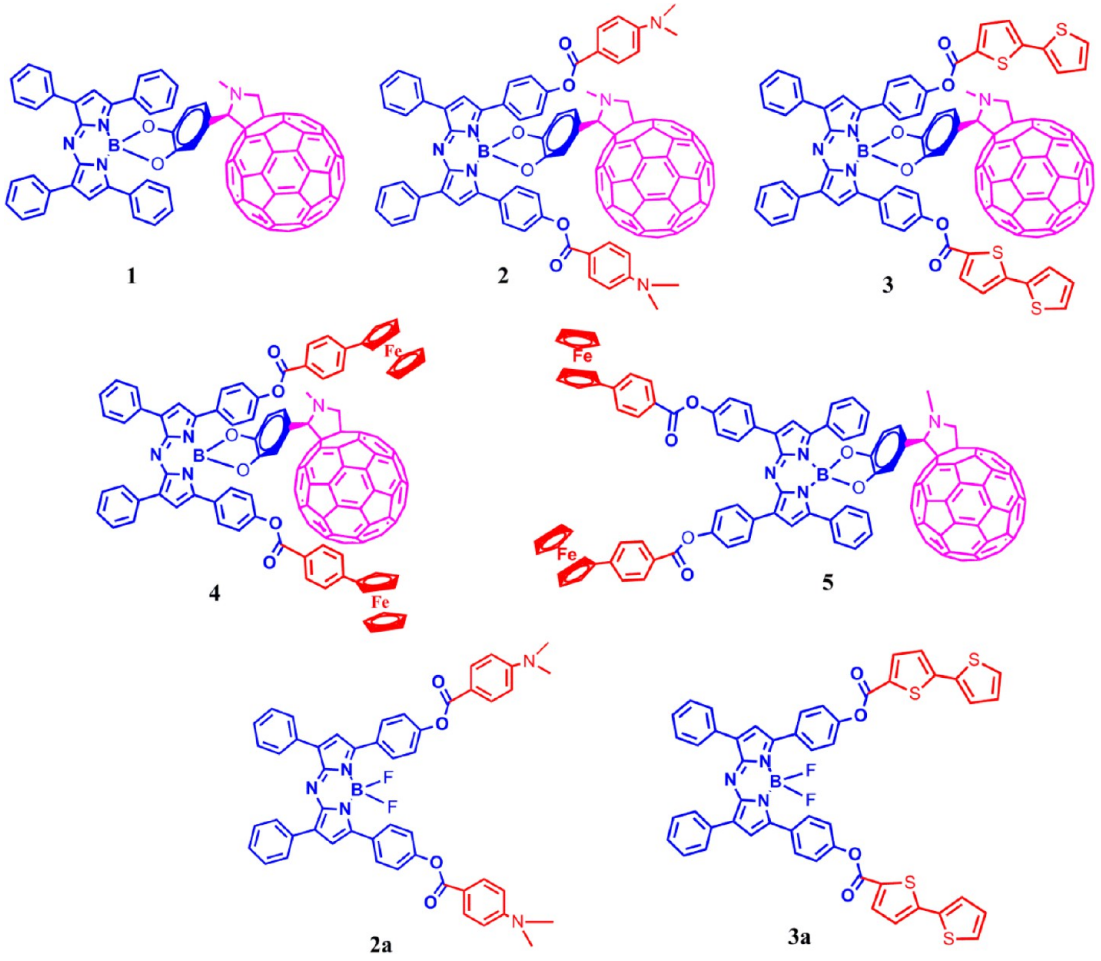

[a]Compounds **2a** and **3a** are control compounds used in the investigation.

photoinduced electron transfer from ferrocene to singlet excited azaBODIPY was observed.[21a] Alternatively, when C_{60} was covalently linked to azaBODIPY (compound **1** in Scheme 1), electron transfer leading to the formation of azaBODIPY$^{\bullet+}$−$C_{60}^{\bullet-}$ was observed.[21c] Excitation transfer was observed when either chlorophyll/porphyrin derivatives or BODIPY was covalently or supramolecularly assembled to azaBODIPY.[21b,22a] Interestingly, when a bisporphyrin was covalently linked to azaBODIPY, the resulting "molecular clip" supramolecularly assembled C_{60} via metal−ligand coordination. In this supramolecular assembly, control over energy- and electron-transfer events was possible to accomplish.[21d] Furthermore, by a combination of zinc porphyrin, BODIPY, and azaBODIPY, a novel broad-band-capturing and -emitting supramolecular triad useful for energy harvesting and building optoelectronic devices was recently reported.[21e] In an azaBODIPY−BODIPY−C_{60} triad, occurrence of photoinduced energy- and electron-transfer events have been reported.[22c] Supramolecular donor−acceptor hybrids of zinc phthalocyanine−azaBODIPY and zinc naphthalocyanine−azaBODIPY, that is, near-infrared absorbing/emitting entities, were recently constructed to observe photoinduced electron-transfer events in the near-infrared region.[21f]

By synthesizing novel bisferrocene−azaBODIPY−fullerene tetrads (compounds **4** and **5** in Scheme 1), occurrence of excitation-wavelength-dependent photochemical events was also reported recently.[23] In these tetrads, azaBODIPY acted as a photosensitizing electron acceptor along with the fullerene, while the ferrocene entities acted as electron donors. Formation of a Fc^{+}−azaBODIPY−$C_{60}^{\bullet-}$ charge-separated state was successfully demonstrated upon C_{60} excitation, whereas Fc^{+}−azaBODIPY$^{\bullet-}$−C_{60} was formed upon azaBODIPY excitation. Encouraged by these findings, in the present study, we have extended our approach of multimodular construction of donor−acceptor tetrads by replacing the ferrocene units of **4** by donors such as *N*,*N*-dimethylaminophenyl (compound **2** in Scheme 1) or bithiophene (compound **3**). The photochemical properties have been compared with those of the azaBODIPY−C_{60} dyad, **1**,[21c] bisferrocene−azaBODIPY−fullerene tetrads, **4** and **5**,[23] and the control triads, **2a** and **3a**, lacking fullerene to understand the role of the spatially close to the acceptor secondary electron donors (ferrocene, dimethylaminophenyl, or bisthiophene) in governing the photochemical events.

RESULTS AND DISCUSSION

Syntheses of Bisdonor−azaBODIPY−Fullerene Supramolecular Tetrads and X-ray Structure of 3a. The syntheses of the supramolecular systems involved a multistep procedure, as shown in Scheme 2, and the details are given in the Experimental Section. Briefly, 1-(4-hydroxyphenyl)-3-

dx.doi.org/10.1021/jp4112469 | J. Phys. Chem. C 2014, 118, 2321−2332

Scheme 2. Synthetic Procedure Adapted for Bisdonor−azaBODIPY−Fullerene Supramolecular Tetrads

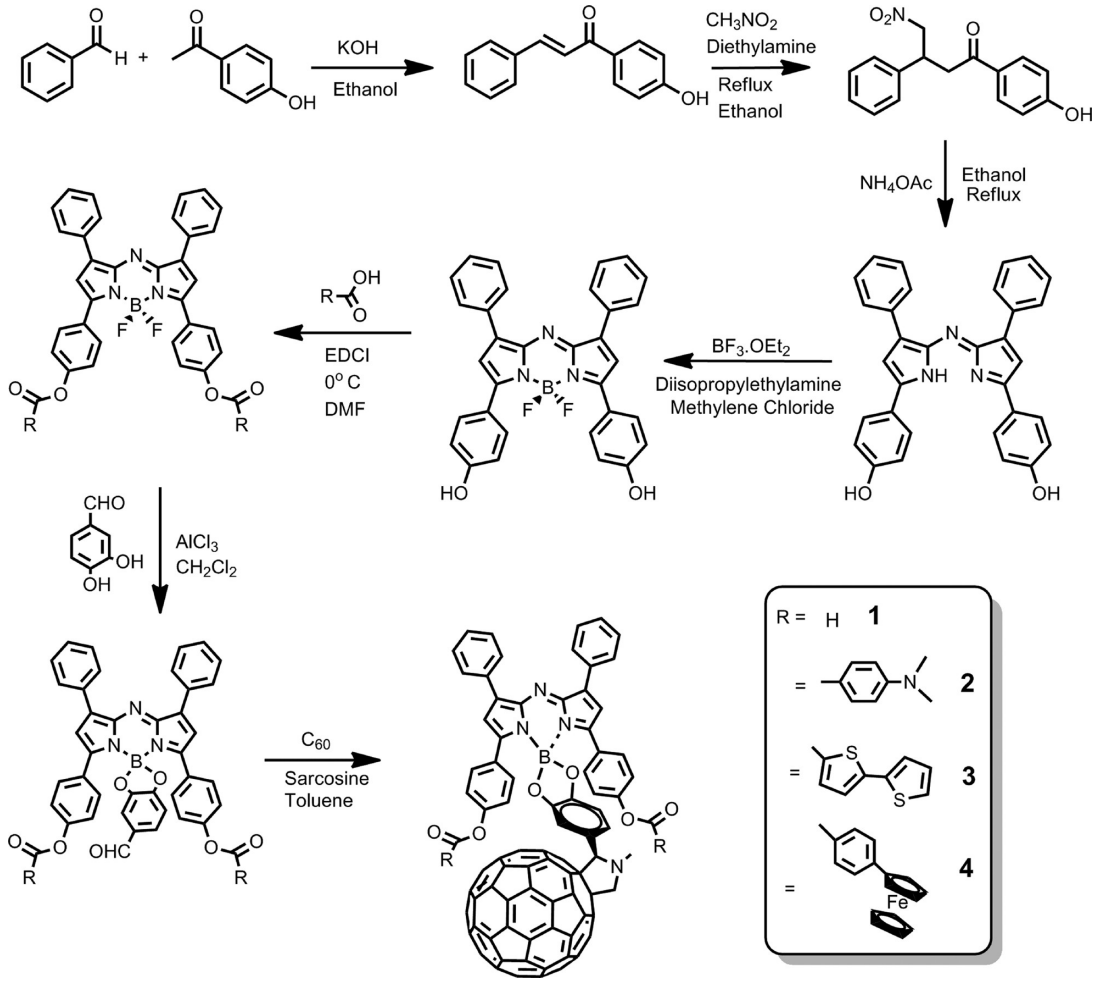

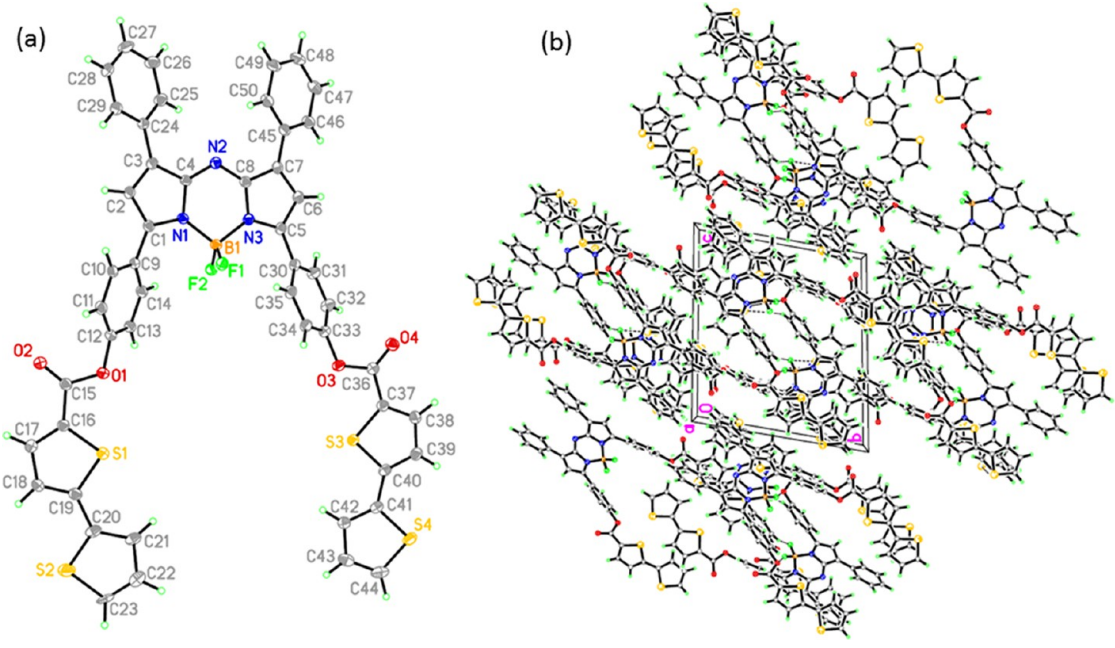

Figure 1. (a) Projection diagram with 50% thermal ellipsoids and (b) the crystal packing diagram of bis(bithiophene)-appended azaBODIPY, **3a**.

phenylpropenone was synthesized from a reaction involving benzaldehyde, 4-hydroxyacetophenone, and potassium hydroxide.[23] This compound was subsequently reacted with nitromethane and diethylamine in dry ethanol to obtained 1-(4-

dx.doi.org/10.1021/jp4112469 | J. Phys. Chem. C 2014, 118, 2321−2332

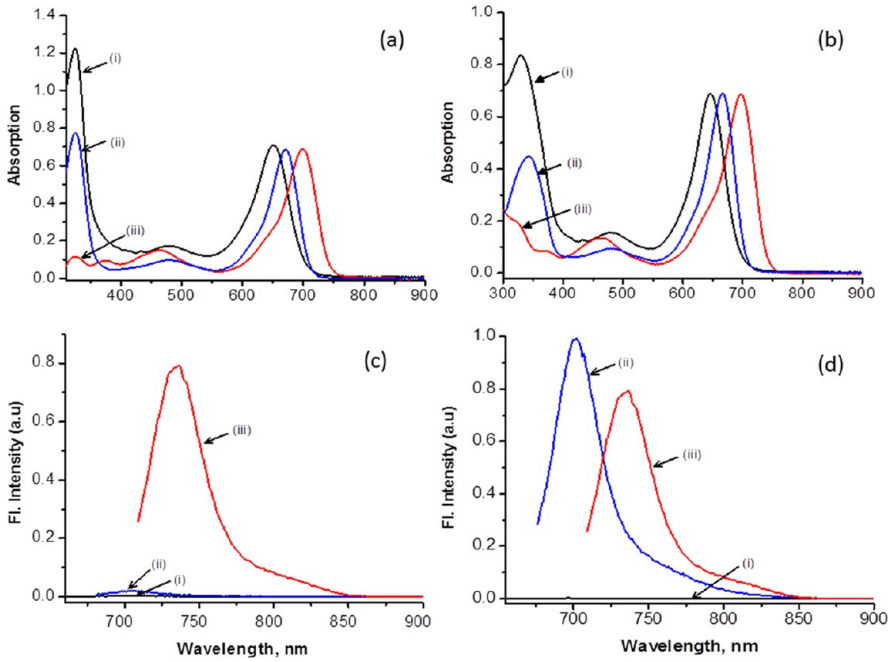

Figure 2. Absorbance (a,b) and emission spectra (c,d) of (i) bisdonor−azaBODIPY−fullerene tetrad (donor = *N*,*N*-dimethylaminophenyl or bithiophene), (ii) bisdonor−azaBODIPY triad, and (iii) bis(4-hydroxyphenyl)azaBODIPY (8.0 μM) in benzonitrile. The azaBODIPYs were excited at the corresponding near-IR peak maxima.

hydroxyphenyl)-4-nitro-3-phenylbutan-1-one. The [5-(4-hydroxyphenyl)-3-phenyl-1*H*-pyrrol-2-yl]-[5-(4-hydroxyphenyl)-3-phenylpyrrol-2-ylidene]amine was synthesized by the reactions of 1-(4-hydroxyphenyl)-4-nitro-3-phenylbutan-1-one with ammonium acetate in ethanol. Next, the BF_2-chelated [5-(4-hydroxyphenyl)-3-phenyl-1*H*-pyrrol-2-yl]-[5-(4-hydroxyphenyl)-3-phenylpyrrol-2-ylidene] amine was synthesized by the reaction of [5-(4-hydroxyphenyl)-3-phenyl-1*H*-pyrrol-2-yl]-[5-(4-hydroxyphenyl)-3-phenylpyrrol-2-ylidene]amine with diisopropylethylamine and boron trifluoride diethyl etherate in dry CH_2Cl_2. Following this, the bisdonor-linked azaBODIPY was obtained by reaction of the BF_2-chelated [5-(4-hydroxyphenyl)-3-phenyl-1*H*-pyrrol-2-yl]-[5-(4-hydroxyphenyl)-3-phenylpyrrol-2-ylidene] amine with appropriate amounts of either *N*,*N*-dimethylaminobenzoic acid (for compound **2a**) or 2,2′-bithiophene-5-carboxylic acid (for compound **3a**) in the presence of *N*-(3-dimethylaminopropyl)-*N*′-ethylcarbodiimide hydrochloride (EDCl) followed by chromatographic purification. These compounds were further reacted with 3,4-dihydroxybenzaldehyde in the presence of $AlCl_3$ to obtain the formyl phenyl dioxyboron derivatives. Finally, fullerene was appended by reacting the purified products obtained from previous steps with fullerene and *N*-methylglycine (sarcosine) in toluene according to Prato's method[24] to obtain compounds **2** and **3**, respectively. The structural integrity of the newly synthesized compounds was established from ^{1}H NMR, mass, and optical techniques.

The X-ray structure and packing diagram of one of the intermediates, bis(bithiophene)-appended azaBODIPY, **3a**, are shown in Figure 1. The molecule crystallized in the triclinic crystal system (space group *P*-1; see the Experimental Section for structure details).[25] In accordance with the earlier structure of azaBODIPY derivatives,[21f,23] the boron assumed a tetrahedral geometry with the two ring nitrogen atoms and two fluorine atoms. One of the bithiophene units was polymorphed in two of the three analyzed crystals. The center-to-center distance between bisthiophene and azaBODIPY was about 13.5 Å. The dihedral angles between heterocycles S1/S2 and S3/S4 were 8.53(8) and 15.26(6)°, respectively, and the two bithiophene units were about 8.9 Å away from each other. Some intermolecular interactions were also observed in the crystal packing. The atomic coordinates, bond lengths, anisotropic displacement parameters, and hydrogen coordinates are given in the Supporting Information (see Tables S1−S4).

Steady-State Absorption and Fluorescence Measurements. Figure 2a and b shows the absorption spectra of the investigated compounds in benzonitrile. The most intense band of azaBODIPY was located in the range of 640−720 nm depending upon the substituents on the aromatic rings. A less intense band in the 465−485 nm region was also observed. The peak maxima of the precursor azaBODIPY, ([5-(4-hydroxyphenyl)-3-phenyl-1*H*-pyrrol-2-yl]-[5-(4-hydroxyphenyl)-3-phenylpyrrol-2-ylidene]amine), was located at 700 nm. This band revealed a blue shift of nearly 30−35 nm upon bis(dimethylaminophenyl) or bis(bithiophene) substitution. The dimethylaminophenyl and bithiophene peaks appeared at 325 and 342 nm, respectively. An additional blue shift of ∼15 nm was witnessed upon fullerene functionalization through the boron center of azaBODIPY. The characteristic sharp peak of fulleropyrrolidine at 430 nm was also observed for both tetrads. The fullerene band was overlapped with the azaBODIPY and bisdonor entities in the UV region and appeared in the 326−328 nm range. The systematic blue shift is suggestive of some intramolecular interactions between the entities in the tetrads.

The steady-state fluorescence emission studies were indicative of the occurrence of excited-state events in the tetrads. The control azaBODIPY revealed an emission band at 735 nm. This band was quenched over 98% for compounds derived from dimethylaminophenyl-functionalized azaBODIPYs, suggesting an electron-transfer event from the electron-donating dimethylaminophenyl to the singlet azaBODIPY, as reported previously for ferrocene-functionalized compounds **4**

dx.doi.org/10.1021/jp4112469 | *J. Phys. Chem. C* 2014, 118, 2321−2332

and **5**.[23] Interestingly, although emission of azaBODIPY is quenched fully in tetrad **3**, the bis(bithiophene)-functionalized ^{1}azaBODIPY* (**3a**) emission was not quenched by electron transfer an/or energy transfer due to energetic considerations, as will be shown in the electrochemical section. In order to verify the role of bithiophene on the fluorescence behavior, additional control experiments were performed. As shown in Figure S1 (Supporting Information), bisthiophene revealed an emission band at 408 nm. In the bis(bithiophene)-functionalized azaBODIPY, **3a**, this band was completely quenched, while by further scanning the wavelength in the longer wavelength range, azaBODIPY emission at 694 nm was observed. A control azaBODIPY lacking bithiophene entities under these experimental conditions revealed an emission band of azaBODIPY at 716 nm whose intensity was about 1/3 of that observed for bis(bithiophene)-derivatized azaBODIPY. These results are indicative of excited-state energy transfer from ^{1}bithiophene* to azaBODIPY in bis(bithiophene)-derivatized azaBODIPY, **3a**.[26] It may be mentioned here that excitation of bithiophene in compound **3** revealed no appreciable emission from either bithiophene or azaBODIPY entities, suggesting occurrence of further photochemical events from ^{1}azaBODIPY* to the appended fullerene.

Electrochemistry and Computational Studies. In order to probe the redox reactivity and establish energy levels, electrochemical studies were performed using the differential pulse voltammetry (DPV) technique. Figure 3 shows DPVs of

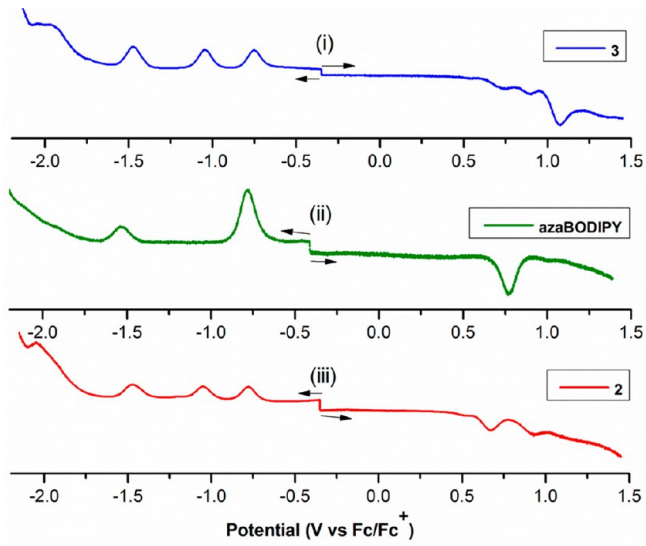

Figure 3. Differential pulse voltammograms of (i) the bis(bithiophene)azaBODIPY–fullerene tetrad (**3**), (ii) azaBODIPY, and (iii) the bis(*N*,*N*-diphenylaminophenyl)azaBODIPY–fullerene tetrad (**2**) in benzonitrile and 0.1 M (n-Bu_4N)ClO_4. Scan rate = 5 mV/s; pulse width = 0.25 s; pulse height = 0.025 V.

the tetrads **2** and **3** along with azaBODIPY in benzonitrile and 0.1 M (n-Bu_4N)ClO_4, while the redox data along with the compounds shown in Scheme 1 are summarized in Table 1. The azaBODIPY revealed one-electron reduction and one-electron oxidation processes located at −0.79 and 0.80 V versus Fc/Fc$^+$, respectively. A second reduction at −1.54 V was also observed. The electrochemical behavior of tetrads **2** and **3** in the negative potential range were similar for the first three one-electron reductions, located at −0.76, −1.05, and −1.47 V versus Fc/Fc$^+$, respectively. By comparison with the reduction potentials of pristine azaBODIPY and fulleropyrrolidine, the first reduction was assigned to the reduction of the azaBODIPY entity, while the second reduction was assigned for the first reduction of fulleropyrrolidine. The third reduction located at −1.47 V was an overlap of second reductions of azaBODIPY and fulleropyrrolidine entities. In the positive potential window, the first and second oxidation was observed for tetrad **2** at 0.66 and 0.93 V, respectively. The former one was ascribed to the overlap between the first oxidation of *N*,*N*-dimethylaminophenyl and azaBODIPY entities, while the latter one represents the second E_{ox} for the azaBODIPY entity. For tetrad **3**, the first oxidation corresponding to azaBODIPY appeared to be a split wave at 0.74 and 0.90 V, while the bithiophene oxidation appeared at 1.08 V versus Fc/Fc$^+$. Multipotential cycling of **3** revealed some film formation; the details are not discussed in the present study.

Figure 4 shows the B3LYP/3-21G(*) optimized structures and molecular electrostatic potential (MEP) maps of tetrads **2** and **3**.[27,28] The structures were completely optimized on a Born–Oppenheimer potential energy surface. In the optimized structures, the azaBODIPY segments were found to be flat with a slight tilt of the peripheral heterocyclic rings, in agreement with the X-ray structure shown in Figure 1. The two donor entities linked to azaBODIPY formed molecular clip type structures to interact with the fullerene entity linked through the central boron atom. The MEP maps revealed the electron-rich and -deficient portions of the tetrads. In agreement with the electrochemical studies, the electron-rich nature of the dimethylaminophenyl over bisthiophene and the electron-deficient nature of the azaBODIPY and fullerene entities in these tetrads are clearly recognized in Figure 4c and d.

The energies of the charge separation were calculated using the redox, geometric, and optical data according to Rehm–Weller's approach,[29] and the calculated values are given in Table 1. The generation of $D^{\bullet+}$–azaBODIPY$^{\bullet-}$–C_{60} and $D^{\bullet+}$–azaBODIPY–$C_{60}^{\bullet-}$ were found to be exergonic via the singlet excited state of azaBODIPY in benzonitrile for **2**; however, for **3**, formation of (bithiophene)$_2$–azaBODIPY$^{\bullet+}$–$C_{60}^{\bullet-}$ via ^{1}azaBODIPY* seems to be the only charge separation pathway. On the basis of the redox potential measurements, the formation of azaBODIPY$^{\bullet-}$–$C_{60}^{\bullet+}$ (∼2.0 eV) is excluded because of its higher energy compared with the ^{1}azaBODIPY* (1.85 eV) and $^1C_{60}$* (1.75 eV) excited states.

Photochemistry. Femtosecond and nanosecond transient absorption spectroscopy were employed to obtain further insights into the excited-state events of the investigated compounds and to corroborate the proposed electron-transfer processes. Toward this end, the investigated tetrads and their control compounds **2a**, **3a**, and azaBODIPY were probed with 390 nm excitation to selectively excite the azaBODIPY fluorophore. The femtosecond transient absorption spectra of azaBODIPY in benzonitrile (Figure S2, Supporting Information) revealed the instantaneous formation of the azaBODIPY singlet excited-state features. Here, the transient absorption spectra were dominated by the formation of the absorption bands of the azaBODIPY singlet state in the visible region at 527 and 823 nm ($k = 3.9 \times 10^8$ s^{-1}). The spectra also revealed pronounced bleaching between 670 and 740 with a maximum at 708 nm ($k = 3.8 \times 10^8$ s^{-1}), which is due to depletion of the singlet ground state. AzaBODIPY singlet excited-state features were long-lived (i.e., 2.6 ns). Implicit was a relatively slow intersystem crossing to the corresponding triplet state of azaBODIPY.

dx.doi.org/10.1021/jp4112469 | J. Phys. Chem. C 2014, 118, 2321–2332

Table 1. Electrochemical Redox Potentials (V versus Fc/Fc$^+$), Free-Energy Change for Charge Separation (ΔG^S_{CS}) for the Bisdonor−azaBODIPY Tetrads in Benzonitrile

compound	$C_{60}^{\bullet-}/C_{60}$	azaBODIPY$^{\bullet-}$/azaBODIPY	$D^{\bullet+}/D$	azaBODIPY$^{\bullet+}$/azaBODIPY	$-\Delta G^S_{CS}$ [a]/ eV	ref
azaBODIPY		−0.79		0.80		21c
1	−1.06	−0.81		0.76, 0.94	0.03[b]	21c
2	−1.05	−0.76	0.66	0.68, 0.93	0.11,[b] 0.42,[c] 0.14[d]	this work
3	−1.05	−0.77	1.08	0.74, 0.90	0.06[e]	this work
4	−1.07	−0.80	0.02	0.68	1.07,[c] 0.80[d]	23
5	−1.07	−0.81	0.05	0.65	1.09,[c] 0.83[d]	23

[a] $\Delta G^S_{CS} = \Delta E_{0-0} - \Delta G_{CR}$, where ΔE_{0-0} is the energy of the lowest excited states of azaBODIPY, being 1.85 eV in benzonitrile. $-\Delta G_{CR} = e(E_{ox} - E_{red})$, where the electrostatic interaction was neglected in benzonitrile. [b]For formation of azaBODIPY$^{\bullet+}$−$C_{60}^{\bullet-}$ via ^{1}azaBODIPY*. [c]For formation of $D^{\bullet+}$−azaBODIPY$^{\bullet-}$−C_{60} via ^{1}azaBODIPY* (D = *N*,*N*-dimethylaminophenyl or ferrocene). [d]For formation of $D^{\bullet+}$−azaBODIPY−$C_{60}^{\bullet-}$ via ^{1}azaBODIPY* (D = *N*,*N*-dimethylaminophenyl or ferrocene). [e]For formation of (bithiophene)$_2$−azaBODIPY$^{\bullet+}$−$C_{60}^{\bullet-}$ via ^{1}azaBODIPY*.

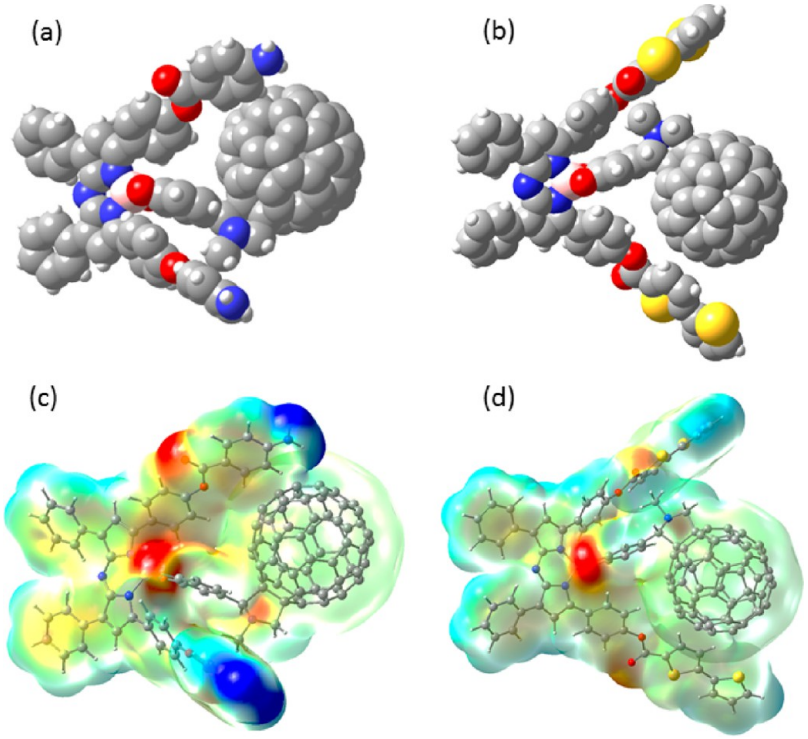

Figure 4. (a) B3LYP/3-21G(*) optimized structures of (a) bis(*N*,*N*-diphenylaminophenyl)−azaBODIPY−fullerene (**2**) and (b) bis(bithiophene)−azaBODIPY−fullerene (**3**) tetrads. (c,d) Their corresponding MEP maps.

The spectral features in the visible region, which were seen immediately (i.e., 5 ps) after excitation of **2a** in PhCN (Figure 5), were virtually the same as those recorded for the azaBODIPY singlet excited state (^{1}azaBODIPY*). The singlet state of azaBODIPY decayed with a rate constant of 2.5×10^{10} s^{-1}, which is much faster than that of the azaBODIPY control, indicating the occurrence of fast and efficient electron transfer from the electron-donating dimethylaminophenyl moiety to ^{1}azaBODIPY* generating (dimethylaminophenyl)$^{\bullet+}$−(azaBODIPY)$^{\bullet-}$. The electron-transfer products in the visible region are hidden under the strong bleaching of the singlet azaBODIPY. This observation is in a good agreement with the steady-state emission studies (Figure 2). From the decay of the singlet excited state of **2a** and azaBODIPY, the rate constant of charge separation was determined to be 2.5×10^{10} s^{-1}.

The transient spectral features observed for **3a** (Figure S3, Supporting Information) were also nearly the same as those recorded for the azaBODIPY singlet excited state (^{1}azaBODIPY*). The singlet decay was found to be 3.3×10^8 s^{-1}, which is about the same as that of azaBODIPY, indicating inefficient, if any, electron transfer from the bithiophene moiety to ^{1}azaBODIPY*. This observation is in a good agreement with the steady-state emission and electrochemical studies.

In the case of tetrad **2**, the spectral features in the visible and near-IR region showed the fast decay of the ^{1}azaBODIPY* (4.0×10^{11} s^{-1}) at 640 nm, which was faster than that of **2a** (Figure 6). This observation suggests that the electron transfer occurs between the azaBODIPY and the closely located C_{60} but not between the azaBODIPY and the dimethylaminophenyl entity. The D−azaBODIPY$^{\bullet+}$−$C_{60}^{\bullet-}$ could further undergo a hole shift reaction to yield $D^{\bullet+}$−azaBODIPY−$C_{60}^{\bullet-}$ as the final charge separation product. The rate constant of charge separation was determined to be 4.0×10^{11} s^{-1}. This was confirmed by recording the quick formation of the fingerprint absorption band of the C_{60} radical anion at 1000 nm. The broad transient absorption at around 900 nm, which decayed

dx.doi.org/10.1021/jp4112469 | J. Phys. Chem. C 2014, 118, 2321−2332

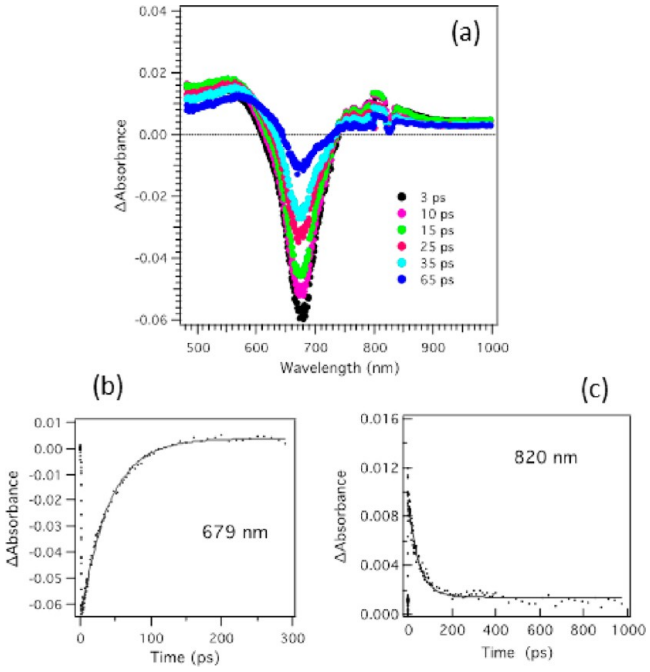

Figure 5. (Upper) Differential absorption spectra obtained upon femtosecond flash photolysis (λ_{ex} = 390 nm) of **2a** in PhCN at the indicated time intervals. (Lower) Time profiles of the singlet excited azaBODIPY at 679 and 820 nm.

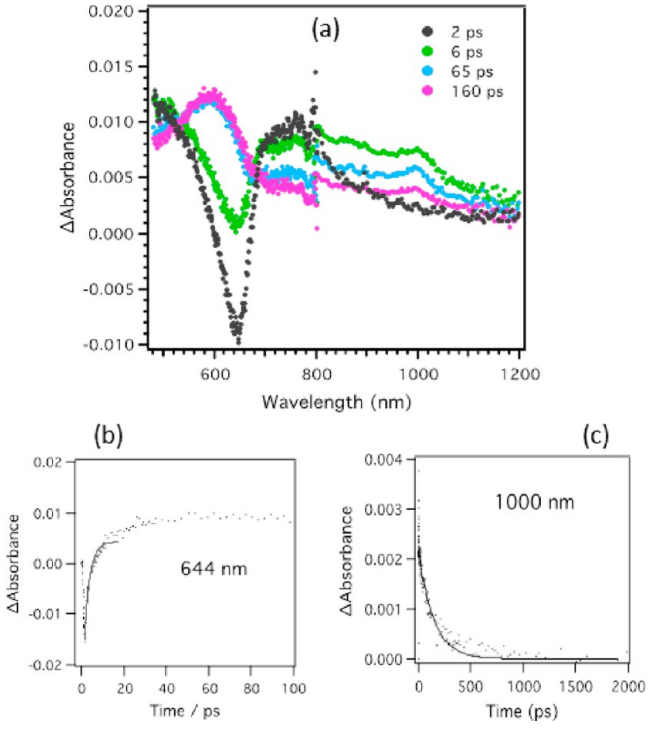

Figure 6. (a) Differential absorption spectra obtained upon femtosecond flash photolysis (λ_{ex} = 390 nm) of tetrad **2** in PhCN at the indicated time intervals. Time−absorption profiles of the C_{60} radical anion at 1000 nm monitoring charge separation and the singlet excited state of azaBODIPY (644 nm), are shown in (b) and (c), respectively.

concomitantly with the transient absorption at 1000 nm due to $C_{60}^{\bullet-}$, can be assigned to azaBODIPY$^{\bullet+}$.[21c] The rate constant of azaBODIPY$^{\bullet+}$ and $C_{60}^{\bullet-}$ recombination was determined to be 6.5 × 10^9 s^{-1}, from which the lifetime of the charge-separated state was determined to be 153 ps. The finding that the lifetimes of the charge-separated states of **1** and **2** are almost the same suggests inefficient hole shift from azaBODIPY$^{\bullet+}$ to D.

In the case of tetrad **3**, the spectral features in the visible and near-IR region showed clear evidence of fast and efficient charge separation (∼1 ps) from the bis(bithiophene)−azaBODIPY moiety to C_{60} (Figure 7). From the decay profile

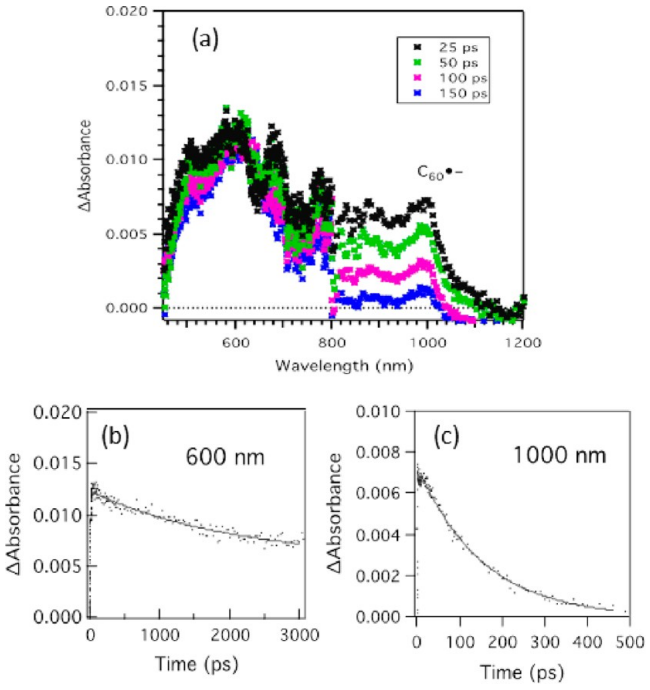

Figure 7. (a) Differential absorption spectra obtained upon femtosecond flash photolysis (λ_{ex} = 390 nm) of tetrad **3** in PhCN at the indicated time intervals. Time−absorption profiles of the C_{60} radical anion at 1000 nm,monitoring charge separation and the triplet state of **3** (600 nm) are shown in (b) and (c), respectively.

of the C_{60} radical anion at 1000 nm, the rate constant of charge recombination was found to be 6.4 × 10^9 s^{-1}. From the k_{CR}, the lifetime of the charge-separated state was estimated to be 160 ps. The absorption band at 700 nm may correspond to the azaBODIPY−bisbithiphene radical cation, while the absorption bands at 450 and 600 nm, which are accompanied by the decay of the C_{60} radical anion, may be attributed to the triplet excited state of azaBODIPY.

The complementary nanosecond transient spectrum showed weak absorption of the triplet excited state of azaBODIPY in the 400−550 nm region for both tetrads (Figures S4 and S5, Supporting Information). This observation suggests that the charge recombination takes place to populate the triplet excited state of azaBODIPY (∼1 eV) as well as the ground state.[21] The proposed energy diagrams for photochemical events occurring upon excitation of the azaBODIPY moiety in **2a** and **2** are summarized in Figure 8, while a similar diagram could be envisioned for the tetrad **3**.

The kinetic data on charge separation and charge recombination for the dyad **1** and tetrads **2**−**5** are listed in Table 2. The k_{CS} of tetrad **3** tracked that of the dyad **1**, indicating little or no influence from the bisthiophene entities; however, k_{CS} of **2** tracked that of **4** and **5**. The k_{CR} values of tetrads **2** and **3** with donor entities in close proximity to the

dx.doi.org/10.1021/jp4112469 | J. Phys. Chem. C 2014, 118, 2321−2332

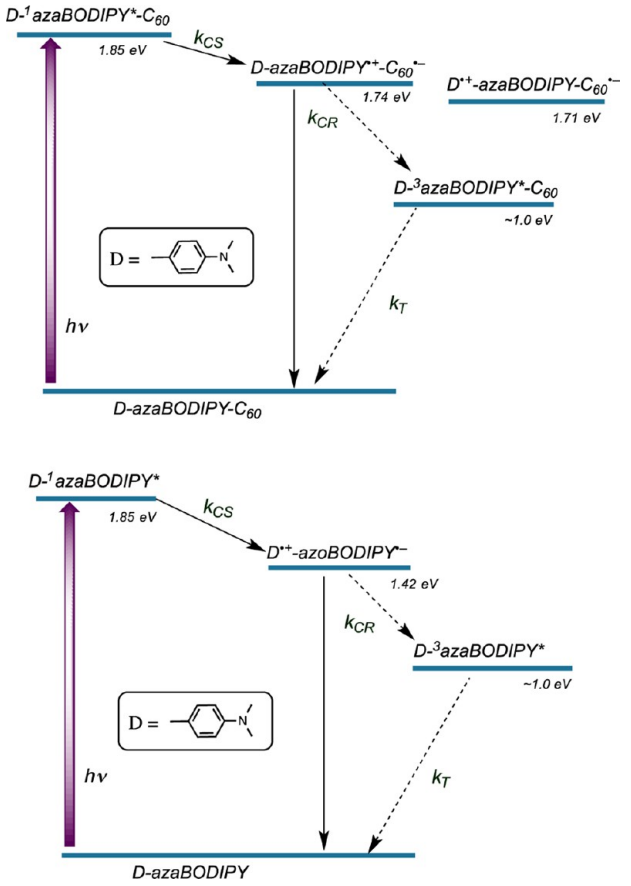

Figure 8. Energy level diagrams showing different photochemical events of tetrad **2** (top) and triad **2a** (bottom). The solid arrows show most likely processes, and dashed arrows show less likely processes.

Table 2. Charge Separation (k_{CS}) and Charge Recombination Rate Constants (k_{CR}) for the Bisdonor−azaBODIPY−Fullerene Supramolecular Systems in Benzonitrile

compound	k_{CS}/s^{-1}	k_{CR}/s^{-1}	ref
1	1.0×10^{12}	5.0×10^{9}	21c
2	4.0×10^{11}	6.5×10^{9}	this work
3	1.0×10^{12}	6.4×10^{9}	this work
4	3.8×10^{11}	8.4×10^{10}	23
5	3.2×10^{11}	1.1×10^{10}	23

electron acceptor, the fullerene, were close to that reported for dyad **1**,[21c] indicating that the final charge-separated states are the same in these tetrads.

CONCLUSIONS

In summary, two tetrads featuring near-IR-emitting sensitizer azaBODIPY, covalently linked to an electron acceptor, the fullerene, and two electron-donor entities, namely, *N*,*N*-dimethylaminophenyl or bithiophene, were designed and synthesized (tetrads **2** and **3**), and the results were compared to the earlier-reported bisferrocene−azaBODIPY−fullerene tetrads (tetrads **4** and **5**). In these tetrads, the position of the donor entities was held close to the fullerene entity. The X-ray structure of one of the precursor triads, bis(bithiophene)−azaBODIPY, was solved to visualize the spatial disposition of the bithiophene moieties with respect to azaBODIPY, while B3LYP/3-21G(*) calculations were performed to visualize the geometric and electronic structures of the tetrads. Free-energy calculations using redox, spectral, and geometry parameters predicted exothermic photoinduced electron transfer, more so for tetrad **2** than for **3**. Subsequently, studies performed using femtosecond transient absorption studies revealed occurrence of ultrafast electron transfer leading to the formation of the D−azaBODIPY$^{\bullet+}$−$C_{60}^{\bullet-}$ radical ion pair in the case of **2** as a major electron-transfer product followed by fast charge recombination as a result of close disposition of the entities. Due to the photophysical similarities of tetrad **3** to the azaBODIPY−fullerene dyad, **1**, the charge separation in this tetrad is primarily attributed to involving the azaBODIPY and fullerene entities with little or no influence from the bithiophene entities. Nanosecond transient absorption studies showed that charge recombination in both tetrads involved populating the triplet excited state of azaBODIPY, as well as the ground state.

EXPERIMENTAL SECTION

Chemicals. All the reagents were obtained from Aldrich Chemicals (Milwaukee, WI), while the bulk solvents utilized in the syntheses were from Fischer Chemicals (Plano, TX). Tetra-*n*-butylammonium perchlorate, (*n*-Bu_4N)ClO_4, used in electrochemical studies was obtained from Fluka Chemicals (Ronkonkoma, NY). The general synthesis of azaBODIPY derivatives was performed according to the procedure reported by O'Shea and co-workers[18] with needed modifications, while Scheme 2 provides the adopted synthetic route of the new compounds. Synthetic details of compounds **1**, **4**, and **5** are given elsewhere.[21c,23]

Synthesis of Precursor azaBODIPY Compounds. *Preparation of 1-(4-Hydroxyphenyl)-3-phenylpropenone.* Benzaldehyde (2.1 g, 2×10^{-2} mol), 4-hydroxyacetophenone (2.69 g, 2×10^{-2} mol), and potassium hydroxide (0.03 g, 6×10^{-4} mol) were dissolved in ethanol/water (85:15 v/v, 100 mL) and stirred at room temperature for a period of 24 h. The reaction mixture was allowed to cool in an ice−water bath during which the product precipitated. Filtration of the reaction mixture gave a pale white solid product (85% yield, 3.81 g); ^{1}H NMR (300 MHz, $CDCl_3$) δ = 7.99−8.04 (m, 2H), 7.77−7.84 (m, 1H), 7.60−7.68, (m, 2H), 7.5−7.58 (m, 1H), 7.39−7.45 (m, 3H), 6.9−6.97 (m, 2H) ppm.

Preparation of 1-(4-Hydroxyphenyl)-4-nitro-3-phenylbutan-1-one. 1-(4-Hydroxyphenyl)-3-phenylpropenone (5.0 g, 2.2×10^{-2} mol), nitromethane (13.61 g, 0.223 mol), and diethylamine (8.12 g, 0.111 mol) were dissolved in dry ethanol (35 mL) and heated under reflux for 24 h. The solution was cooled and acidified with 1 M HCl to precipitate the compound (72% yield, 4.58 g); ^{1}H NMR (300 MHz, $CDCl_3$) δ = 7.82 (d, J = 8.48 Hz, 2H), 7.2−7.34 (m, 5H), 6.8 (d, J = 8.5 Hz, 2H), 4.8−4.83 (m, 1H), 4.62−4.7 (m, 1H), 4.15−4.2 (m, 1H), 3.35−3.4 (m, 2H) ppm.

Preparation of [5-(4-Hydroxyphenyl)-3-phenyl-1H-pyrrol-2-yl]-[5-(4-hydroxyphenyl)-3-phenylpyrrol-2-ylidene]amine. 1-(4-Hydroxyphenyl)-4-nitro-3-phenylbutan-1-one (5 g, 1.8×10^{-2} mol) and ammonium acetate (47.31 g, 0.61 mol) and ethanol (125 mL) were heated under reflux for 24 h. During the course of the reaction, the product precipitated as a blue−black solid. The reaction was allowed to cool to room temperature, and the solid was filtered and washed with ethanol to give the product (51% yield, 2.16 g); ^{1}H NMR (300 MHz, $CDCl_3$) δ = 8.04 (d, J = 6.62 Hz, 4H), 7.84 (d, 4H), 7.32−7.4 (m, 6H), 7.12 (s, 2H), 6.98 (d, J = 8.69 Hz, 4H) ppm.

dx.doi.org/10.1021/jp4112469 | J. Phys. Chem. C 2014, 118, 2321−2332

Preparation of BF_2-Chelated [5-(4-Hydroxyphenyl)-3-phenyl-1H-pyrrol-2-yl]-[5-(4-hydroxyphenyl)-3-phenylpyrrol-2-ylidene]amine. [5-(4-Hydroxyphenyl)-3-phenyl-1*H*-pyrrol-2-yl]-[5-(4-hydroxy-phenyl)-3-phenylpyrrol-2-ylidene]amine (1 g, 2.07 mmol) was dissolved in dry CH_2Cl_2 (100 mL). Diisopropylethylamine (2.71 g, 2.1×10^{-2} mol) and boron trifluoride diethyl etherate (4.16 g, 2.9×10^{-2} mol) were added, and the mixture was stirred at room temperature under N_2 for 24 h. The mixture was washed with water, and the organic layer was separated, dried over Na_2SO_4, and evaporated to dryness. The residue was purified by column chromatography on silica gel with CH_2Cl_2/ethyl acetate 4:1 to give a metallic red solid (69% yield, 0.76 g); ^{1}H NMR (400 MHz, $CDCl_3$) δ = 8.1−8.15 (m, 8H), 7.35−7.45 (m, 6H), 7.18 (s, 2H), 6.9−6.93 (m, 4H) ppm. MS(MALDI TOF); *m*/*z*: $C_{32}H_{22}BF_2N_3O_2$, calcd: 529.18; found: 529.39.

Synthetic Procedure for $(DMAP)_2$−azaBODIPY−C_{60}, 2.

*Synthesis of $(DMAP)_2$−azaBODIPY, **2a**.* 4-Dimethylaminobenzoic acid (82 mg, 0.5 mmol) was dissolved in (15 cm^3) DMF, to which EDCI (113 mg, 0.58 mmol) was added at 0 °C under N_2, followed by the addition of BF_2-chelated [5-(4-hydroxyphenyl)-3-phenyl-1*H*-pyrrol-2-yl]-[5-(4-hydroxyphenyl)-3-phenylpyrrol-2-ylidene]amine (52 mg, 0.1 mmol), after which the mixture was stirred for 24h. Then, the solvent was removed under reduced pressure. The residue was dissolved in CH_2Cl_2, and the mixture was washed with water. The organic layer was separated and dried over Na_2SO_4, and the solvent was evaporated. The residue was purified by column chromatography on silica gel with CH_2Cl_2/hexanes (1:1) to give compound **2a**: yield 20 mg (25%); ^{1}H NMR (400 MHz, $CDCl_3$) δ = 8.15 (d, 4H), 8.04 (d, 4H), 7.90 (m, 2H), 7.80 (m, 4H), 7.42 (m, 4H), 7.30 (d, 2H), 7.04 (s, 2H), 6.82 (m, 6H), 3.02 (m, 12H) ppm. UV/vis (λ_{max}) 671 nm in benzonitrile.

Synthesis of $(DMAP)_2$−azaBODIPY−aldehyde. $(DMAP)_2$−azaBODIPY from the previous step (20 mg, 0.24 mmol) was dissolved in (10 cm^3) dry CH_2Cl_2 and stirred under argon for 10 min. Then, $AlCl_3$ (4.85 mg, 0.36 mmol) was added, and the solution was further stirred for 15 min before addition of 3,4-dihydroxybenzaldehyde (5.03 mg, 0.36 mmol). The mixture was stirred for 20 min, and the solvent was evaporated under reduced pressure. The crude product was purified by column chromatography (deactivated basic alumina) with CH_2Cl_2/hexanes 1:1 to give the product: yield 0.008 g (36%); ^{1}H NMR (400 MHz, $CDCl_3$) δ = 9.62 (s, 1H), 8.12 (d, 4H), 8.04 (m, 8H), 7.46 (m, 8H), 7.34 (d, 4H), 7.04 (s, 2H), 6.98 (s, 1H), 6.68 (m, 4H), 3.02 (s, 12H) ppm.

*Synthesis of $(DMAB)_2$−azaBODIPY−C_{60}, **2**.* To a solution of C_{60} (35 mg, 0.048 mmol), in dry toluene (60 cm^3), were added sarcosine (7.24 mg, 0.081 mmol) and the $(DMAB)_2$−azaBODIPY−aldehyde (15 mg, 0.016 mmol). The solution mixture was refluxed for 24 h, and the solvent was removed under vacuum. The residue was purified by column chromatography (silica) with 3:7 ethyl acetate/toluene as the eluent to give the product: yield 0.008 g (40%); ^{1}H NMR (400 MHz, $CDCl_3$) δ = 8.10 (m, 6H), 7.98 (d, 2H), 7.70 (m, 2H), 7.42 (m, 10H), 6.80 (m, 4H), 6.60 (m, 6H), 6.20 (m, 1H), 4.82 (d, 1H), 4.62 (s, 1H), 4.20 (d, 1H), 3.04 (m, 12H), 2.60 (s, 3H) ppm. UV/vis (λ_{max}) 650 nm in benzonitrile. MALDI TOF-MS (dichloromethane); *m*/*z*: $C_{119}H_{49}BN_6O_6$, calcd: 1668.38; found: two fragments 949.16 ($C_{59}H_{51}BN_6O_6$) and 802.12 ($C_{50}H_{42}$ BN_5O_5).

Synthetic Procedure for $(Bithio)_2$−azaBODIPY−C_{60}, 3.

*Synthesis of $(Bithio)_2$−azaBODIPY, **3a**.* 2,2′-Bithiophene-5-carboxylic acid (294 mg, 1.4 mmol) was dissolved in (20 cm^3) DMF, to which EDCI (321 mg, 1.67 mmol) was added at 0 °C under N_2, followed by the addition of compound BF_2-chelated [5-(4-hydroxyphenyl)-3-phenyl-1*H*-pyrrol-2-yl]-[5-(4-hydroxyphenyl)-3-phenylpyrrol-2-ylidene]amine (148 mg, 0.28 mmol), after which the mixture was stirred for 24 h. Then, the solvent was removed under reduced pressure. The residue was dissolved in CH_2Cl_2, and the mixture was washed with water. The organic layer was separated and dried over Na_2SO_4, and the solvent was evaporated. The residue was purified by column chromatography on silica gel with CH_2Cl_2/hexanes (1:1) to give compound **3a**: yield 57 mg (22%); ^{1}H NMR (400 MHz, $CDCl_3$) δ = 8.12 (d, 4H), 8.06 (d, 4H), 7.88 (d, 2H), 7.45 (m, 6H), 7.38 (d, 4H), 7.32 (d, 4H), 7.20 (d, 2H), 7.05 (m, 4H) ppm. UV/vis (λ_{max}) 666 nm in benzonitrile. MALDI TOF-MS (dichloromethane); *m*/*z*: $C_{50}H_{30}BF_2N_3O_4S_4$, calcd: 913.12; found: 913.27.

Synthesis of $(Bithio)_2$−azaBODIPY−Aldehyde. $(Bithio)_2$−azaBODIPY (57 mg, 0.06 mmol) was dissolved in (10 cm^3) dry CH_2Cl_2 and stirred under argon for 10 min. Then, $AlCl_3$ (12.4 mg, 0.09 mmol) was added, and the solution was further stirred for 15 min before addition of 3,4-dihydroxybenzaldehyde (13 mg, 0.09 mmol). The mixture was stirred for 20 min, and the solvent was evaporated under reduced pressure. The crude product was purified by column chromatography (deactivated basic alumina) with CH_2Cl_2/hexanes 1:1.5 to give the product: yield 0.043g (68%); ^{1}H NMR (400 MHz, $CDCl_3$) δ = 9.62 (s, 1H), 8.02 (d, 4H), 7.89 (d, 2H), 7.45 (m, 6H), 7.38 (m, 6H), 7.20 (d, 2H), 7.02 (m, 4H), 6.81 (m, 6H), 6.62 (s, 1H), 6.22 (d, 2H) ppm.

*Synthesis of $(Bithio)_2$−azaBODIPY−C_{60}, **3**.* To a solution of C_{60} (91.7 mg, 0.12 mmol), in dry toluene (200 cm^3), were added sarcosine (19 mg, 0.21 mmol) and the $(bithio)_2$−azaBODIPY−aldehyde (43 mg, 0.04 mmol). The solution mixture was refluxed for 24 h, and the solvent was removed under vacuum. The residue was purified by column chromatography (silica) with 3:7 ethyl acetate/toluene as the eluent to give the product: yield 0.020 g (28%); ^{1}H NMR (400 MHz, $CDCl_3$) δ = 8.02 (d, 4H), 7.62 (m, 2H), 7.40 (m, 8H), 7.28 (m, 4H), 7.18 (m, 4H), 7.04 (m, 6H), 6.82 (m, 3H), 6.18 (m, 2H), 4.84 (d, 1H), 4.62 (s, 1H), 4.20 (d, 1H), 2.60 (s, 3H) ppm. UV/vis (λ_{max}) 645 nm in benzonitrile. MALDI TOF-MS (dichloromethane); *m*/*z*: $C_{119}H_{39}BN_4O_6S_4$, calcd: 1758.18; found: two fragments 1039.29 ($C_{59}H_{40}BN_4O_6S_4$) and 847.22 ($C_{50}H_{39}BN_4O_5S_2$).

Spectral Measurements. The UV−visible spectral measurements were carried out with a Shimadzu Model 2550 double monochromator UV−visible spectrophotometer. The fluorescence emission was monitored by using a Varian Eclipse spectrometer. A right angle detection method was used. The ^{1}H NMR studies were carried out on a Varian 400 MHz and 300 MHz spectrometer. Tetramethylsilane (TMS) was used as an internal standard. Differential pulse voltammograms were recorded on an EG&G PARSTAT electrochemical analyzer using a three-electrode system. A platinum button electrode was used as the working electrode. A platinum wire served as the counter electrode, and a Ag/AgCl electrode was used as the reference electrode. A ferrocene/ferrocenium redox couple was used as an internal standard. All of the solutions were purged prior to electrochemical and spectral measurements using argon gas. Matrix-assisted laser desorption/ionization time-of-flight mass spectra (MALDI TOF) were measured on a Kratos Compact MALDI I (Shimadzu) for the metal complex in

dx.doi.org/10.1021/jp4112469 | J. Phys. Chem. C 2014, 118, 2321−2332

PhCN with dithranol used as a matrix. The computational calculations were performed by DFT B3LYP/3-21G* methods with the GAUSSIAN 03 software package on high-speed PCs.

X-ray Structural Data (3a). The X-ray diffraction examination for compound **3a** was carried out using a Bruker SMATR APEX2 CCD-based X-ray diffractometer equipped with a low-temperature cryostat (Oxford Instruments) and a Mo target X-ray tube (λ = 0.71073 Å). Empirical formula: $C_{50}H_{30}BF_2N_3O_4S_4$; formula weight: 913.82; temperature: 100(2) K; crystal system: triclinic; space group: *P*-1. Unit cell dimensions: a = 9.2474(9) Å, b = 14.3754(14) Å, c = 16.4018(16) Å, α = 98.841(1)°, β = 102.721(1)°, γ = 94.087(1)°. Volume: 2089.0(4) Å^3; Z: 2; density (calculated): 1.453 Mg/m^3; absorption coefficient: 0.289 mm^{-1}; F(000): 940; crystal size: 0.24 × 0.12 × 0.08 mm^3; θ range for data collection: 1.76−27.06°. Index ranges: $-11 \le h \le 11$, $-18 \le k \le 18$, $-20 \le l \le 20$; reflections collected: 25342; independent reflections: 9095 [R(int) = 0.0329]; completeness to θ: 27.06°, 99.3%; absorption correction: semiempirical from equivalents; max. and min. transmission: 0.9775 and 0.9338; refinement method: full-matrix least-squares on F^2; data/restraints/parameters: 9095/15/587; goodness-of-fit on F^2: 1.009. Final R indices: [$I > 2\sigma(I)$] $R1$ = 0.0401, $wR2$ = 0.0936; R indices (all data): $R1$ = 0.0573, $wR2$ = 0.1026. Largest diff. peak and hole: 0.620 and −0.530 e·Å^{-3}.

Laser Flash Photolysis. The studied compounds were excited by a Panther OPO pumped by a Nd:YAG laser (Continuum, SLII-10, 4−6 ns fwhm) with the powers of 1.5 and 3.0 mJ/pulse. The transient absorption measurements were performed using a continuous xenon lamp (150 W) and an InGaAs-PIN photodiode (Hamamatsu 2949) as a probe light and a detector, respectively. The output from the photodiodes and a photomultiplier tube was recorded with a digitizing oscilloscope (Tektronix, TDS3032, 300 MHz).

Femtosecond transient absorption spectroscopy experiments were conducted using an ultrafast source, Integra-C (Quantronix Corp.), an optical parametric amplifier, TOPAS (Light Conversion Ltd.), and a commercially available optical detection system, Helios provided by Ultrafast Systems LLC. The sources for the pump and probe pulses were derived from the fundamental output of Integra-C (780 nm, 2 mJ/pulse and fwhm = 130 fs) at a repetition rate of 1 kHz. 75% of the fundamental output of the laser was introduced into TOPAS, which has optical frequency mixers resulting in a tunable range from 285 to 1660 nm, while the rest of the output was used for white light generation. Typically, 2500 excitation pulses were averaged for 5 s to obtain the transient spectrum at a set delay time. Kinetic traces at appropriate wavelengths were assembled from the time-resolved spectral data. All measurements were conducted at 298 K. The transient spectra were recorded using fresh solutions in each laser excitation.

■ ASSOCIATED CONTENT

Ⓢ Supporting Information

Fluorescence spectra of control compounds, femtosecond transient spectra of azaBODIPY and **3a**, nanosecond transient spectrum of **2** and **3**, and complete X-ray structural data for **3a**. This material is available free of charge via the Internet at http://pubs.acs.org.

■ AUTHOR INFORMATION

Corresponding Authors

*E-mail: fukuzumi@chem.eng.osaka-u.ac.jp (S.F.).

*E-mail: Francis.DSouza@UNT.edu. Fax: 940-565-4318 (F.D.).

Present Address

⊥M.E.E.-K.: Department of Chemistry, Faculty of Science, Kafrelsheikh University, Egypt

Notes

The authors declare no competing financial interest.

■ ACKNOWLEDGMENTS

This work was supported by National Science Foundation (Grant No. 1110942 to F.D.), the Global COE (center of excellence) program "Global Education and Research Center for Bio-Environmental Chemistry" of Osaka University from the Ministry of Education, Culture, Sports, Science and Technology, Japan, and GRL (2010-00353) and WCU (R31-2008-000-10010-0) from KOSEF/MEST, Korea.

■ REFERENCES

(1) (a) Gust, D.; Moore, T. A.; Moore, A. L. Solar Fuels via Artificial Photosynthesis. *Acc. Chem. Res.* **2009**, *42*, 1890−1898. (b) Gust, D.; Moore, T. A.; Moore, A. L. Mimicking Photosynthetic Solar Energy Transduction. *Acc. Chem. Res.* **2001**, *34*, 40−48.

(2) Wasielewski, M. R. Self-Assembly Strategies for Integrating Light Harvesting and Charge Separation in Artificial Photosynthetic Systems. *Acc. Chem. Res.* **2009**, *42*, 1910−1921.

(3) (a) Bottari, G.; de la Torre, G.; Guldi, D. M.; Torres, T. Covalent and Noncovalent Phthalocyanine−Carbon Nanostructure Systems: Synthesis, Photoinduced Electron Transfer, and Application to Molecular Photovoltaics. *Chem. Rev.* **2010**, *110*, 6768−6816. (b) Guldi, D. M.; Rahman, G. M. A.; Sgobba, V.; Ehli, C. Multifunctional Molecular Carbon Materials—From Fullerenes to Carbon Nanotubes. *Chem. Soc. Rev.* **2006**, *35*, 471−487. (c) Schuster, D. I.; Li, K.; Guldi, D. M. Porphyrin−Fullerene Photosynthetic Model Systems with Rotaxane and Catenane Architectures. *C. R. Chimie* **2006**, *9*, 892−908.

(4) (a) Satake, A.; Kobuke, Y. Artificial Photosynthetic Systems: Assemblies of Slipped Cofacial Porphyrins and Phthalocyanines Showing Strong Electronic Coupling. *Org. Biomol. Chem.* **2007**, *5*, 1679−1691. (b) Delgado, J. L.; Herranz, M. Á.; Martín, N. The Nano-Forms of Carbon. *J. Mater. Chem.* **2008**, *18*, 1417−1426. (c) Tasis, D.; Tagmatarchis, N.; Bianco, A.; Prato, M. Chemistry of Carbon Nanotubes. *Chem. Rev.* **2006**, *106*, 1105−1136.

(5) (a) Sessler, J. L.; Lawrence, C. M.; Jayawickramarajah, J. Molecular Recognition via Base-Pairing. *Chem. Soc. Rev.* **2007**, *36*, 314−325. (b) Fukuzumi, S.; Ohkubo, K.; D'Souza, F.; Sessler, J. L. Supramolecular Electron Transfer by Anion Binding. *Chem. Commun.* **2012**, *48*, 9801−9815.

(6) (a) Umeyama, T.; Imahori, H. Carbon Nanotube-Modified Electrodes for Solar Energy Conversion. *Energy Environ. Sci.* **2008**, *1*, 120−133. (b) Hasobe, T. Supramolecular Nanoarchitectures for Light Energy Conversion. *Phys. Chem. Chem. Phys.* **2010**, *12*, 44−57. (c) Imahori, H.; Umeyama, T.; Kei, K.; Yuta, T. Self-Assembling Porphyrins and Phthalocyanines for Photoinduced Charge Separation and Charge Transport. *Chem. Commun.* **2012**, *48*, 4032−4045.

(7) (a) D'Souza, F.; Ito, O. Photoinduced Electron Transfer in Supramolecular Systems of Fullerenes Functionalized with Ligands Capable of Binding to Zinc Porphyrins and Zinc Phthalocyanines. *Coord. Chem. Rev.* **2005**, *249*, 1410−1422. (b) D'Souza, F.; Ito, O. Supramolecular Donor−Acceptor Hybrids of Porphyrins/Phthalocyanines with Fullerenes/Carbon Nanotubes: Electron Transfer, Sensing, Switching, and Catalytic Applications. *Chem. Commun.* **2009**, 4913−4928. (c) El-Khouly, M. E.; Ito, O.; Smith, P. M.; D'Souza, F. Intermolecular and Supramolecular Photoinduced Electron Transfer Processes of Fullerene−Porphyrin/Phthalocyanine Systems. *J. Photochem. Photobiol. C* **2004**, *5*, 79−104. (d) D'Souza, F.; Ito, O. Photosensitized Electron Transfer Processes of Nanocarbons Applicable to Solar Cells. *Chem. Soc. Rev.* **2012**, *41*, 86−96. (e) D'Souza, F.;

Ito, O. Recent Advances in Photoinduced Electron Transfer Processes of Fullerene-Based Molecular Assemblies and Nanocomposites. *Molecules* **2012**, *17*, 5816−5835.
(8) (a) Fukuzumi, S. New Perspective of Electron Transfer Chemistry. *Org. Biomol. Chem.* **2003**, *1*, 609−620. (b) Fukuzumi, S. Bioinspired Electron-Transfer Systems and Applications. *Bull. Chem. Soc. Jpn.* **2006**, *79*, 177−195. (c) Fukuzumi, S. Development of Bioinspired Artificial Photosynthetic Systems. *Phys. Chem. Chem. Phys.* **2008**, *10*, 2283−2297. (d) Fukuzumi, S.; Kojima, T. Photofunctional Nanomaterials Composed of Multiporphyrins and Carbon-Based π-Electron Acceptors. *J. Mater. Chem.* **2008**, *18*, 1427−1439. (e) Fukuzumi, S.; Honda, T.; Ohkubo, K.; Kojima, T. Charge Separation in Metallomacrocycle Complexes Linked with Electron Acceptors by Axial Coordination. *Dalton Trans.* **2009**, 3880−3889. (f) Fukuzumi, S.; Ohkubo, K. Assemblies of Artificial Photosynthetic Reaction Centres. *J. Mater. Chem.* **2012**, *22*, 4575−4587.
(9) (a) Lewis, N. S.; Nocera, D. G. Powering the Planet: Chemical Challenges in Solar Energy Utilization. *Proc. Natal. Acad. Sci. U.S.A.* **2006**, *103*, 15729−15735. (b) Turner, J. A. A Realizable Renewable Energy Future. *Science* **1999**, *285*, 687−689. (c) Barber, J. Photosynthetic Energy Conversion: Natural and Artificial. *Chem. Soc. Rev.* **2009**, *38*, 185. (d) Scholes, G. D.; Fleming, G. R.; Olaya-Castro, A.; van Grondelle, R. Lessons from Nature about Solar Light Harvesting. *Nat. Chem.* **2011**, *3*, 763−774. (e) Kamat, P. V. Meeting the Clean Energy Demand: Nanostructure Architectures for Solar Energy Conversion. *J. Phys. Chem. C* **2007**, *111*, 2834−2860. (f) Fukuzumi, S. Bioinspired Energy Conversion Systems for Hydrogen Production and Storage. *Eur. J. Inorg. Chem.* **2008**, 1351−1362. (g) Fukuzumi, S.; Yamada, Y. Catalytic Activity of Metal-Based Nanoparticles for Photocatalytic Water Oxidation and Reduction. *J. Mater. Chem.* **2012**, *22*, 24284−24296.
(10) (a) Connolly, J. S., Ed. *Photochemical Conversion and Storage of Solar Energy*; Academic: New York, 1981. (b) *Molecular Level Artificial Photosynthetic Materials*; Meyer, G. J., Ed.; Wiley: New York, 1997. (c) Verhoeven, J. W. From Close Contact to Long-Range Intramolecular Electron Transfer. *Adv. Chem. Phys.* **1999**, *106*, 603−644. (d) Osuka, A.; Mataga, N.; Okada, T. A Chemical Approach towards the Photosynthetic Reaction Centre. *Pure Appl. Chem.* **1997**, *69*, 797−802. (e) Flamigni, L.; Barigelletti, F.; Armaroli, N.; Collin, J.-P.; Dixon, I. M.; Sauvage, J.-P.; Williams, J. A. G. Photoinduced Processes in Multicomponent Arrays Containing Transition Metal Complexes. *Coord. Chem. Rev.* **1999**, *190−192*, 671−682. (f) Diederich, F.; Gomez-Lopez, M. Supramolecular Fullerene Chemistry. *Chem. Rev. Soc.* **1999**, *28*, 263−277. (g) Hammarström, L.; Sun, L.; Akermark, B.; Styring, S. A Biomimetic Approach to Artificial Photosynthesis: Ru(II)−Polypyridine Photo-Sensitisers Linked to Tyrosine and Manganese Electron Donors. *Spectrochim. Acta, Part A* **2001**, *57*, 2145−2160.
(11) (a) Blanco, M.-J.; Consuelo Jimenez, M.; Chambron, J.-C.; Heitz, V.; Linke, M.; Sauvage, J.-P. Rotaxanes as New Architectures for Photoinduced Electron Transfer and Molecular Motions. *Chem. Rev. Soc.* **1999**, *28*, 293−305. (b) Balzani, V.; Ceroni, P.; Juris, A.; Venturi, M.; Campagna, S.; Puntoriero, F.; Serroni, S. Dendrimers Based on Photoactive Metal Complexes. Recent Advances. *Coord. Chem. Rev.* **2001**, *219*, 545−572. (c) Balzani, V.; Credi, A.; Venturi, M. Photochemical Conversion of Solar Energy. *ChemSusChem* **2008**, *1*, 26−58.
(12) (a) Fukuzumi, S.; Ohkubo, K.; Sastre-Santos, Á. Formation of a Long-Lived Charge-Separated State of a Zinc Phthalocyanine−Perylenediimide Dyad by Complexation with Magnesium Ion. *Chem. Commun.* **2005**, 3814−3816. (b) Fukuzumi, S.; Ohkubo, K.; Ortiz, J.; Gutiérrez, A. M.; Fernández-Lázaro, F.; Sastre-Santos, Á. Control of Photoinduced Electron Transfer in Zinc Phthalocyanine−Perylenediimide Dyad and Triad by the Magnesium Ion. *J. Phys. Chem. A* **2008**, *112*, 10744−10752. (c) Céspedes-Guirao, F. J.; Ohkubo, K.; Fukuzumi, S.; Sastre-Santos, Á.; Fernández-Lázaro, F. Synthesis and Photoinduced Electron Transfer of Phthalocyanine−Perylenebisimide Pentameric Arrays. *J. Org. Chem.* **2009**, *74*, 5871−5880. (d) Blas-Ferrando, V. M.; Ortiza, J.; Bouissanea, L.; Ohkubo, K.; Fukuzumi, S.; Fernández-Lázaroa, F.; Sastre-Santos, Á. Rational Design of a Phthalocyanine−Perylenediimide Dyad with a Long-Lived Charge-Separated State. *Chem. Commun.* **2012**, *48*, 6241−6243.
(13) (a) Imahori, H.; Tamaki, K.; Guldi, D. M.; Luo, C.; Fujitsuka, M.; Ito, O.; Sakata, Y.; Fukuzumi, S. Modulating Charge Separation and Charge Recombination Dynamics in Porphyrin−Fullerene Linked Dyads and Triads: Marcus-Normal versus Inverted Region. *J. Am. Chem. Soc.* **2001**, *123*, 2607−2617. (b) Imahori, H.; Guldi, D. M.; Tamaki, K.; Yoshida, Y.; Luo, C.; Sakata, Y.; Fukuzumi, S. Charge Separation in a Novel Artificial Photosynthetic Reaction Center Lives 380 ms. *J. Am. Chem. Soc.* **2001**, *123*, 6617−6628. (c) Fukuzumi, S.; Ohkubo, K.; Imahori, H.; Shao, J.; Ou, Z.; Zheng, G.; Chen, Y.; Pandey, R. K.; Fujitsuka, M.; Ito, O.; Kadish, K. M. Photochemical and Electrochemical Properties of Zinc Chlorin−C_{60} Dyad as Compared to Corresponding Free-Base Chlorin−C_{60}, Free-Base Porphyrin−C_{60}, and Zinc Porphyrin−C_{60} Dyads. *J. Am. Chem. Soc.* **2001**, *123*, 10676−10683. (d) Takai, A.; Chkounda, M.; Eggenspiller, A.; Gros, C. P.; Lachkar, M.; Barbe, J.-M.; Fukuzumi, S. Efficient Photoinduced Electron Transfer in a Porphyrin Tripod−Fullerene Supramolecular Complex via π−π Interactions in Nonpolar Media. *J. Am. Chem. Soc.* **2010**, *132*, 4477−4489.
(14) (a) El-Khouly, M. E.; Wijesinghe, C. A.; Nesterov, V. N.; Zandler, M. E.; Fukuzumi, S.; D'Souza, F. Ultrafast Photoinduced Energy and Electron Transfer in Multi-Modular Donor−Acceptor Conjugates. *Chem.−Eur. J.* **2012**, *18*, 13844−13853. (b) D'Souza, F.; Maligaspe, E.; Ohkubo, K.; Zandler, M. E.; Subbaiyan, N. K.; Fukuzumi, S. Photosynthetic Reaction Center Mimicry: Low Reorganization Energy Driven Charge Stabilization in Self-Assembled Cofacial Zinc Phthalocyanine Dimer−Fullerene Conjugate. *J. Am. Chem. Soc.* **2009**, *131*, 8787−8797. (c) Fukuzumi, S.; Saito, K.; Kashiwagi, Y.; Crossley, M. J.; Gadde, S.; D'Souza, F.; Araki, Y.; Ito, O. Multiple Photosynthetic Reaction Centres Composed of Supramolecular Assemblies of Zinc Porphyrin Dendrimers with a Fullerene Acceptor. *Chem. Commun.* **2011**, *47*, 7980−7982. (d) Fukuzumi, S.; Saito, K.; Ohkubo, K.; Troiani, V.; Qiu, H.; Gadde, S.; D'Souza, F.; Solladié, N. Multiple Photosynthetic Reaction Centres Using Zinc Porphyrinic Oligopeptide−Fulleropyrrolidine Supramolecular Complexes. *Phys. Chem. Chem. Phys.* **2011**, *13*, 17019−17022.
(15) (a) Treibs, A.; Kreuzer, F. H. Difluoroboryl Complexes of Di- and Tripyrrylmethenes. *Liebigs Ann. Chem.* **1968**, *718*, 208−223. (b) Loudet, A.; Burgess, K. BODIPY Dyes and Their Derivatives: Syntheses and Spectroscopic Properties. *Chem. Rev.* **2007**, *107*, 4891−4932. (c) Boens, N.; Leen, V.; Dehaen, W. Fluorescent Indicators Based on BODIPY. *Chem. Soc. Rev.* **2012**, *41*, 1130−1172. (d) Qian, X.; Xiao, Y.; Xu, Y.; Guo, X.; Qian, J.; Zhu, W. "Alive" Dyes as Fluorescent Sensors: Fluorophore, Mechanism, Receptor and Images in Living Cells. *Chem. Commun.* **2010**, *46*, 6418−6436.
(16) (a) Li, F.; Yang, S. I.; Ciringh, T.; Seth, J.; Martin, C. H., III; Singh, D. L.; Kim, D.; Birge, R. R.; Bocian, D. F.; Holten, D.; Lindsey, J. S. Design, Synthesis, and Photodynamics of Light-Harvesting Arrays Comprised of a Porphyrin and One, Two, or Eight Boron-Dipyrrin Accessory Pigments. *J. Am. Chem. Soc.* **1998**, *120*, 10001−10017.
(17) (a) Ulrich, G.; Ziessel, R.; Harriman, A. The Chemistry of Fluorescent Bodipy Dyes: Versatility Unsurpassed. *Angew. Chem., Int. Ed.* **2008**, *47*, 1184−1201. (b) El-Khouly, M. E.; Fukuzumi, S.; D'Souza, F. Photosynthetic Antenna-Reaction Center Mimicry by Using Boron Dipyrromethene Sensitizers. *ChemPhysChem* **2014**, *15*, 31−47.
(18) (a) Tasior, M.; O'Shea, D. F. BF_2-Chelated Tetraarylazadipyrromethenes as NIR Fluorochromes. *Bioconjugate Chem.* **2010**, *21*, 1130−1133. (b) Gorman, A.; Killoran, J.; O'Shea, C.; Kenna, T.; Gallagher, W. M.; O'Shea, D. F. In Vitro Demonstration of the Heavy-Atom Effect for Photodynamic Therapy. *J. Am. Chem. Soc.* **2004**, *126*, 10619−10631. (c) Hall, M. J.; McDonnell, S. O.; Killoran, J.; O'Shea, D. F. A Modular Synthesis of Unsymmetrical Tetraarylazadipyrromethenes. *J. Org. Chem.* **2005**, *70*, 5571−5578. (d) Grossi, M.; Palma, A.; McDonnell, S. O.; Hall, M. J.; Rai, D. K.; Muldoon, J.; O'Shea, D. F. Mechanistic Insight into the Formation of Tetraarylazadipyrromethenes. *J. Org. Chem.* **2012**, *77*, 9304−9312.

(19) (a) Palma, A.; Tasior, M.; Frimannsson, D. O.; Vu, T. T.; Meallet-Renault, R.; O'Shea, D. F. New On-Bead Near-Infrared Fluorophores and Fluorescent Sensor Constructs. *Org. Lett.* **2009**, *11*, 3638−3641. (b) Murtagh, J.; Frimannsson, D. O.; O'Shea, D. F. Azide Conjugatable and pH Responsive Near-Infrared Fluorescent Imaging Probes. *Org. Lett.* **2009**, *11*, 5386−5389. (c) McDonnell, S. O.; Hall, M. J.; Allen, L. T.; Byrne, A.; Gallagher, W. M.; O'Shea, D. F. Supramolecular Photonic Therapeutic Agents. *J. Am. Chem. Soc.* **2005**, *127*, 16360−16361.

(20) (a) Flavin, K.; Lawrence, K.; Bartelmess, J.; Tasior, M.; Navio, C.; Bittencourt, C.; O'Shea, D. F.; Guldi, D. M.; Giordani, S. Synthesis and Characterization of Boron Azadipyrromethene Single-Wall Carbon Nanotube Electron Donor−Acceptor Conjugates. *ACS Nano* **2011**, *5*, 1198−1206. (b) Yuan, M.; Yin, X.; Zheng, H.; Ouyang, C.; Zuo, Z.; Liu, H.; Li, Y. Light Harvesting and Efficient Energy Transfer in Dendritic Systems: New Strategy for Functionalized Near-Infrared BF_2-Azadipyrromethenes. *Chem.—Asian J.* **2009**, *4*, 707−713. (c) Bouit, P. A.; Kamada, K.; Feneyrou, P.; Berginc, G.; Toupet, L.; Maury, O.; Andraud, C. Two-Photon Absorption-Related Properties of Functionalized BODIPY Dyes in the Infrared Range up to Telecommunication Wavelengths. *Adv. Mater.* **2009**, *21*, 1151−1154. (d) Leblebici, S. Y.; Catane, L.; Barclay, D. E.; Olson, T.; Chen, T. L.; Ma, B. Near-Infrared Azadipyrromethenes as Electron Donor for Efficient Planar Heterojunction Organic Solar Cells. *ACS Appl. Mater. Interfaces* **2011**, *3*, 4469−4474. (e) Flavin, K.; Kopfa, I.; Murtagh, J.; Grossi, M.; O'Shea, D. F.; Giordani, S. Excited State on/off Switching of a Boron Azadipyrromethene Single-Wall Carbon Nanotube Conjugate. Replacing Phenyl Ring with Thiophene: an Approach to Longer Wavelength Aza-Dipyrromethene Boron Difluoride (Aza-BODIPY) Dyes. *Supramol. Chem.* **2012**, *24*, 23−28.

(21) (a) Amin, A. N.; El-Khouly, M. E.; Subbaiyan, N. K.; Zandler, M. E.; Supur, M.; Fukuzumi, S.; D'Souza, F. Syntheses, Electrochemistry, and Photodynamics of Ferrocene−Azadipyrromethane Donor−Acceptor Dyads and Triads. *J. Phys. Chem. A.* **2011**, *115*, 9810−9819. (b) El-Khouly, M. E.; Amin, A. N.; Zandler, M. E.; Fukuzumi, S.; D'Souza, F. Near-IR Excitation Transfer and Electron Transfer in a BF_2-Chelated Dipyrromethane−Azadipyrromethane Dyad and Triad. *Chem.—Eur. J.* **2012**, *18*, 5239−5247. (c) Amin, A. N.; El-Khouly, E.; Subbaiyan, N. K.; Zandler, M. E.; Fukuzumi, S.; D'Souza, F. A novel BF_2-Chelated Azadipyrromethene−Fullerene Dyad: Synthesis, Electrochemistry and Photodynamics. *Chem. Commun.* **2012**, *48*, 206−208. (d) D'Souza, F.; Amin, A. N.; El-Khouly, M. E.; Subbaiyan, N. K.; Zandler, M. E.; Fukuzumi, S. Supramolecular Polyads of Covalently Linked AzaBODIPY Bisporphyrin 'Molecular Clip' Hosting Fullerene. *J. Am. Chem. Soc.* **2012**, *134*, 654−664. (e) Bandi, V.; Ohkubo, K.; Fukuzumi, S.; D'Souza, F. A Broad-Band Capturing and Emitting Molecular Triad: Synthesis and Photochemistry. *Chem. Commun.* **2013**, *49*, 2867−2869. (f) Bandi, V.; El-Khouly, M. E.; Nesterov, V. N.; Karr, P. A.; Fukuzumi, S.; D'Souza, F. Self-Assembled via Metal−Ligand Coordination AzaBODIPY−Zinc Phthalocyanine and AzaBODIPY−Zinc Naphthalocyanine Conjugates: Synthesis, Structure, and Photoinduced Electron Transfer. *J. Phys. Chem. C* **2013**, *117*, 5638−5649.

(22) (a) Kataoka, Y.; Shibata, Y.; Tamiaki, H. Intramolecular Excitation Energy Transfer from Visible Light Absorbing Chlorophyll Derivatives to a Near-IR Light Emitting Boron Dipyromethene Moiety. *Chem. Lett.* **2010**, *39*, 953−955. (b) Shi, W.-J.; Menting, R.; Ermilov, E. A.; Lo, P. C.; Roeder, B.; Ng, D. K. P. Formation and Photoinduced Processes of the Host−Gust Complexes of *β*-Cyclodextrin Conjugated azaBODIPY and Tetrasulfonated Porphyrins. *Chem. Commun.* **2013**, *49*, 5277−5279. (c) Shi, W.-J.; El-Khouly, M. E.; Ohkubo, K.; Fukuzumi, S.; Ng, D. K. P. Photosynthetic Antenna-Reaction Center Mimicry with a Covalently Linked Monostyryl Boron-Dipyrromethene−AzaBODIPY−C_{60} Triad. *Chem.—Eur. J.* **2013**, *19*, 11332−11341.

(23) Bandi, V.; El-Khouly, M. E.; Ohkubo, K.; Nesterov, V. N.; Zandler, M. E.; Fukuzumi, S.; D'Souza, F. Excitation-Wavelength Dependent Ultrafast Photoinduced Electron Transfer in Bisferrocene/BF_2-Chelated-AzaBODIPY/Fullerene Tetrads. *Chem.—Eur. J.* **2013**, *19*, 7221−7230.

(24) Maggini, M.; Scorrano, G.; Prato, M. Addition of Azomethine Ylides to C_{60}: Synthesis, Characterization and Functionalization of Fullerene Pyrrolidines. *J. Am. Chem. Soc.* **1993**, *115*, 9798−9799.

(25) CCDC-943635 contains the supplementary crystallographic data for this paper. These data can be obtained free of charge from The Cambridge Crystallographic Data Centre via www.ccdc.cam.ac.uk/data_-request/cif.

(26) *Principles of Fluorescence Spectroscopy*, 3rd ed.; Lakowicz, J. R., Ed.; Springer: Singapore, 2006.

(27) Frisch, M. J.; Trucks, G. W.; Schlegel, H. B.; Scuseria, G. E.; Robb, M. A.; Cheeseman, J. R.; Zakrzewski, V. G.; Montgomery, J. A.; Stratmann, R. E.; Burant, J. C.; Dapprich, S.; Millam, J. M.; et al. *Gaussian 03*; Gaussian, Inc.: Pittsburgh, PA, 2003.

(28) For a general review on DFT applications of porphyrin−fullerene systems, see: Zandler, M. E.; D'Souza, F. The Remarkable Ability of B3LYP/3-21G(*) Calculations to Describe Geometry, Spectral and Electrochemical Properties of Molecular and Supramolecular Porphyrin−Fullerene Conjugates. *C. R. Chemie* **2006**, *9*, 960−981.

(29) (a) Rehm, D.; Weller, A. Kinetics of Fluorescence Quenching by Electron and Hydrogen-Atom Transfer. *Isr. J. Chem.* **1970**, *7*, 259−271. (b) Mataga, N.; Miyasaka, H. In *Electron Transfer*; Jortner, J., Bixon, M., Eds.; John Wiley & Sons: New York, 1999; Part 2, pp 431−496.